

X-523-66-42

NASA TM X 55421

# ADVANCED POLARIZATION DIVERSITY AUTOTRACK RECEIVER (APDAR) 136 MC SATELLITE TRACKING EVALUATION TESTS

FACILITY FORM 602

N66-19517

(ACCESSION NUMBER)

(THRU)

(PAGES)

(CODE)

TM X 55421

(NASA CR OR TMX OR AD NUMBER)

(CATEGORY)

BY

RALPH E. TAYLOR

GPO PRICE \$ \_\_\_\_\_

CFSTI PRICE(S) \$ \_\_\_\_\_

Hard copy (HC) 2.00Microfiche (MF) .50

ff 653 July 65

FEBRUARY 1, 1966

 NASA

GODDARD SPACE FLIGHT CENTER

GREENBELT, MARYLAND



ADVANCED POLARIZATION DIVERSITY  
AUTOTRACK RECEIVER (APDAR)  
136 MC SATELLITE TRACKING  
EVALUATION TESTS

by  
Ralph E. Taylor

February 1, 1966

Goddard Space Flight Center  
Greenbelt, Maryland



## SUMMARY

19517

The 136 Mc satellite tracking evaluation tests of the advanced polarization diversity autotrack receiver (APDAR) system are discussed. APDAR performance is compared to a conventional 136 Mc autotrack receiver of a type now utilized in STADAN (Satellite Tracking and Data Acquisition Network) by tracking the TIROS VII, IX and X satellites, as well as OSO (S-17). The performance of APDAR, utilizing an automatic polarization tracking feature, has been demonstrated to be superior to a conventional autotrack receiving system utilizing a fixed polarization.

Curry



## TABLE OF CONTENTS

Summary . . . . .	iii
List of Figures . . . . .	vi
INTRODUCTION . . . . .	1
TIROS VII, IX, and X TEST RESULTS . . . . .	2
OSO (S-17) TEST RESULTS . . . . .	15
RF PHASE MEASUREMENTS . . . . .	16
BORESIGHT ANTENNA ROTATION TESTS . . . . .	19
CONCLUSIONS . . . . .	23
ACKNOWLEDGMENTS . . . . .	25
References . . . . .	25





## LIST OF FIGURES

<u>Figure</u>		<u>Page</u>
1	APDAR 6-channel autotrack receiving system for 136 Mc evaluation tests . . . . .	3
2	APDAR 136 Mc test evaluation hookup for linear polarization to Teledyne autotrack receivers . . . . .	4
3	APDAR 136 Mc test evaluation hookup for circular polarization to Teledyne autotrack receivers . . . . .	5
4	TIROS VII 7/23/65 pass. Comparison of APDAR and conventional autotrack receivers . . . . .	6
5	TIROS IX 5/27/65 pass. Comparison of APDAR and conventional autotrack receivers . . . . .	7
6	TIROS IX 5/28/65 pass. Comparison of APDAR and conventional autotrack receivers . . . . .	8
7	TIROS IX 7/19/65 pass. Comparison of ADPAR and conventional autotrack receivers . . . . .	9
8	TIROS X 7/23/65 pass. Comparison of APDAR and conventional autotrack receivers . . . . .	10
9	TIROS IX, vertical (V) and horizontal (H) fading characteristics . . . . .	11
10	OSO (S-17) 6/11/65 pass. Linear receiving polarization . . .	12
11	OSO (S-17) 7/28/65 pass No. 1. Comparison of APDAR and conventional autotrack receivers . . . . .	13
12	OSO (S-17) 7/28/65 pass No. 2. Comparison of APDAR and conventional autotrack receivers . . . . .	14

<u>Figure</u>		<u>Page</u>
13	IMP C APDAR vertical (V) and horizontal (H) phase data. .	18
14	Various polarizations transmitted by a circularly polarized satellite antenna . . . . .	20
15	Boresight antenna test to simulate satellite polarization fading . . . . .	20
16	Boresight antenna rotation test. Linear polarization to Teledyne autotrack receiver . . . . .	21
17	Boresight antenna rotation test. Circular polarization to Teledyne autotrack receiver . . . . .	23

# ADVANCED POLARIZATION DIVERSITY

## AUTOTRACK RECEIVER (APDAR)

### 136 MC SATELLITE TRACKING EVALUATION TESTS

by

Ralph E. Taylor

Goddard Space Flight Center

#### INTRODUCTION

The Advanced Polarization Diversity Autotrack Receiver (APDAR) system utilizes a conventional simultaneous lobing sum-difference type amplitude monopulse autotrack receiving technique, as described by Rhodes (Reference 1). It is refined to include an optimum (maximal ratio) predetection diversity combining technique (Reference 2) to eliminate adverse effects of polarization fading. The APDAR system provides automatic polarization tracking of an incoming radio signal while automatically pointing a space-tracking data acquisition antenna, such as an 85-foot dish, toward the satellite.

APDAR incorporates a multiple phase-lock loop technique (References 3 and 4) that automatically tracks the phase of the respective vertical (V) and horizontal (H) antenna signals, compares phase to a coherent reference, and then provides coherent addition of the V and H signals in a predetection diversity combiner. APDAR also includes an open-loop mode for broad-band, non-coherent signal tracking that utilizes a modified Dicke Radiometer technique to obtain sensitive automatic gain control for autotrack. APDAR thus eliminates the requirement for fixed polarization antenna switching to provide improved autotrack performance.

The recently completed APDAR satellite tracking evaluation tests at 136 Mc utilized the original D. S. Kennedy SATAN\*-type phase-array autotrack antenna located at Bldg. 86 (near Goddard East-gate water tower). The purpose of the

---

\*Satellite Automatic Tracking Antenna.

evaluation was to demonstrate operational feasibility by tracking the TIROS VII, IX, X, and OSO (S-17) and to compare the APDAR performance with that of a conventional amplitude monopulse autotrack receiver utilizing a fixed receiving polarization. Simultaneous Sanborn recordings of both APDAR and conventional autotrack receivers were made during the satellite passes, and detailed results are discussed.

The SATAN antenna polarization coaxial switches (16 total) were removed and the number of comparator RF network coaxial hybrids was reduced from 12 to 8 units to provide separate vertical (V) and horizontal (H) channels for APDAR. The 6-channel APDAR autotrack system shown in Figure 1 was used with the latest integrated comparator RF network. The advanced comparator RF network is more reliable and requires fewer coaxial connectors than existing STADAN units.

The APDAR receiver automatically tracks the incoming antenna polarization, regardless of orientation, by means of a predetection diversity combining technique. In order to compare performance with conventional autotrack, two hookup modes for receiving either linear or circular polarization were incorporated for the Teledyne autotrack receivers (Model 105A) to simulate typical STADAN receiving modes. A simultaneous performance comparison was thus obtained between APDAR and our conventional SATAN autotrack receivers.

The tracking loop bandwidth (1-sided noise b.w.) was set to 100 cps and the automatic gain control (AGC) speed to 30 milliseconds for all of the tests described.

## TIROS VII, IX AND X TEST RESULTS

The TIROS satellites (VII, IX, and X) have circularly polarized transmitting antennas, thus linear polarization (Figure 2) was used for the two Teledyne autotrack receivers connected to receive vertical and horizontal polarization, respectively. The corresponding hookup for circular polarization is shown in Figure 3. The antenna servo was made to separately autotrack with APDAR or either of the two Teledyne units by push-button selection and simultaneous Sanborn recordings were made of AGC and X-Y axis error outputs from all receivers.

Vertical and horizontal fading by as much as 30 db was observed from the conventional autotrack recordings of TIROS VII, IX, and X. Figures 4 through 12 are typical Sanborn recording excerpts. The APDAR X- and Y-axis error



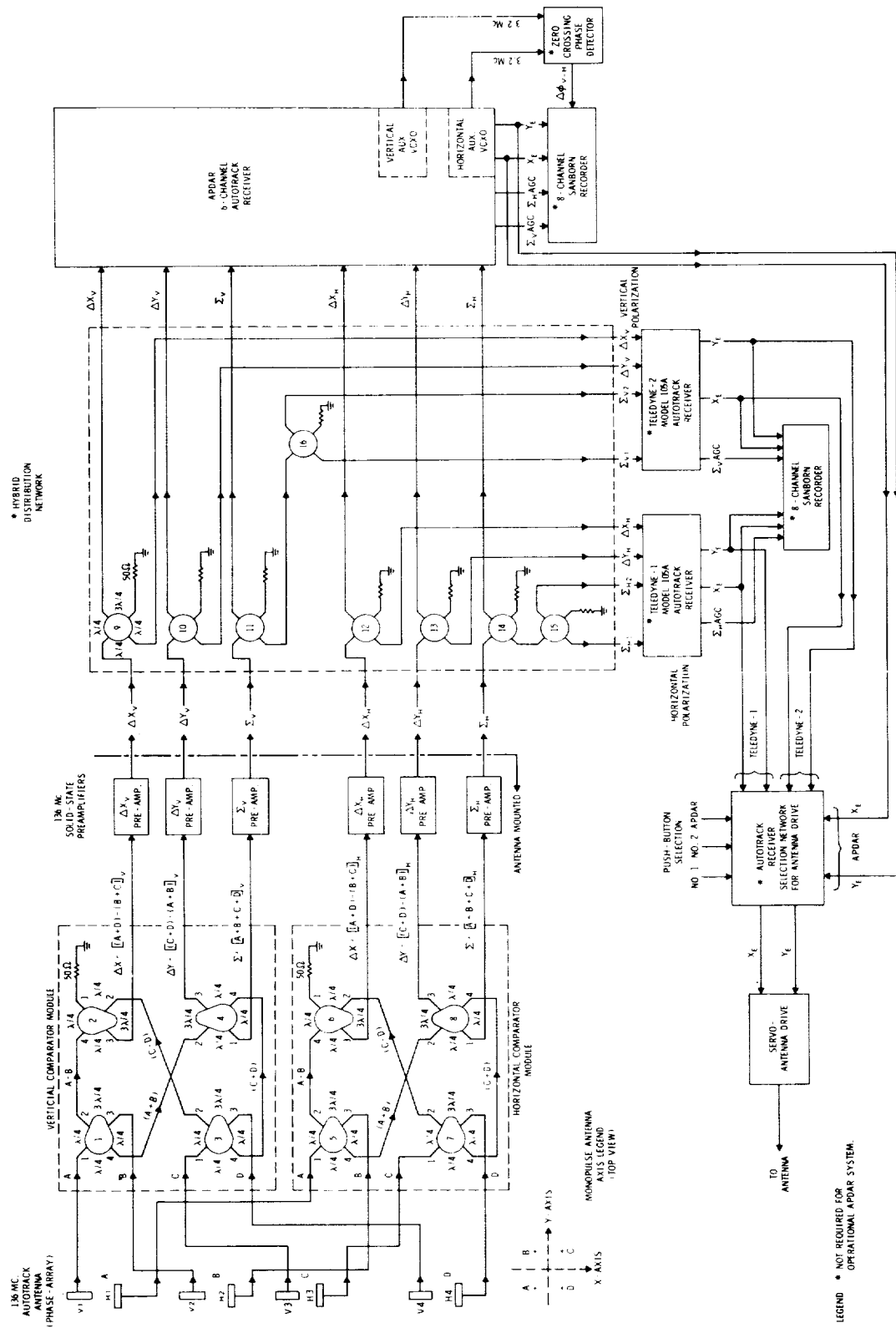


Figure 2-APDAR 136 Mc test evaluation hookup for linear polarization to Teledyne autotrack receivers.

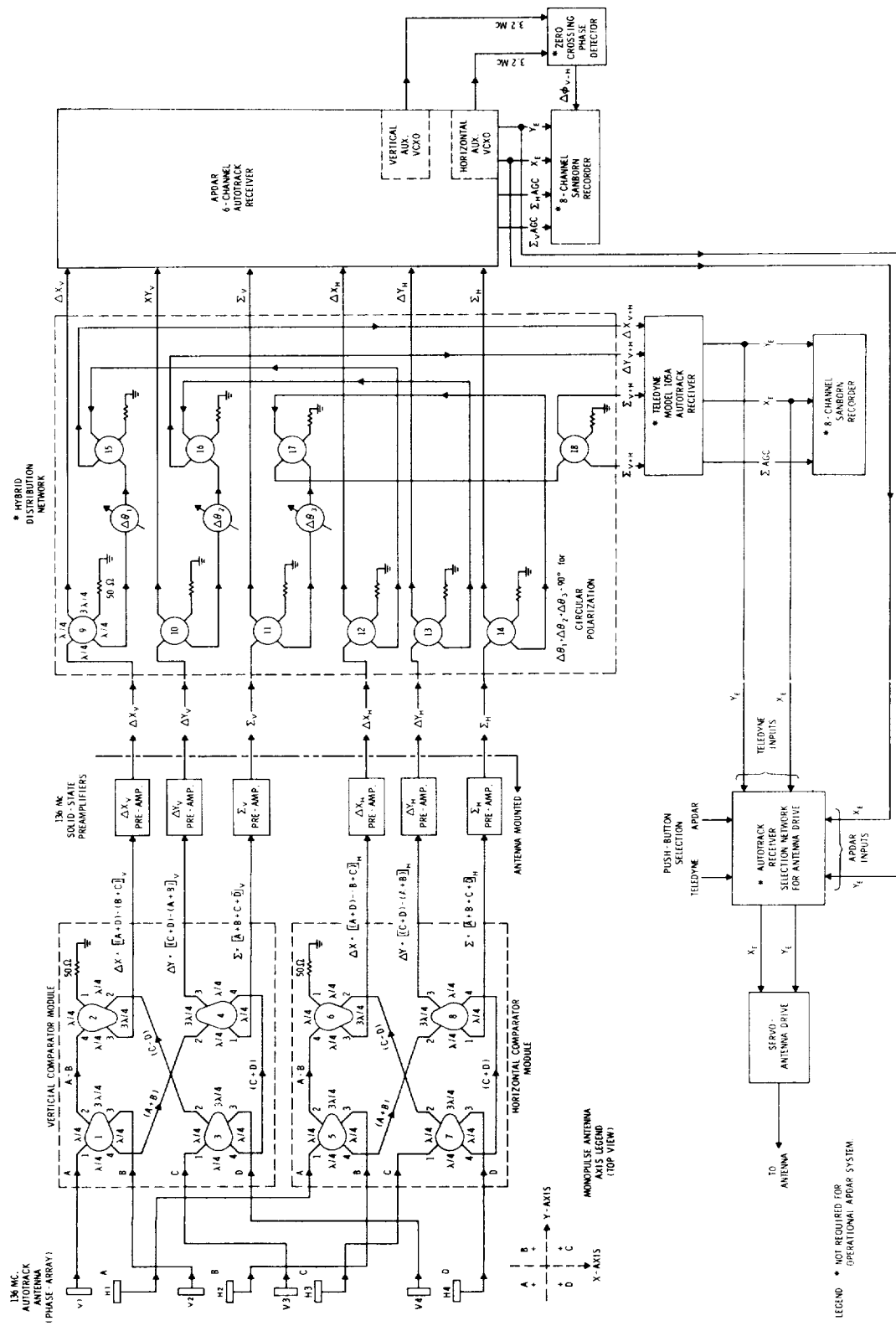


Figure 3-APDAR 136 Mc test evaluation hookup for circular polarization to Teledyne autotrack receivers.

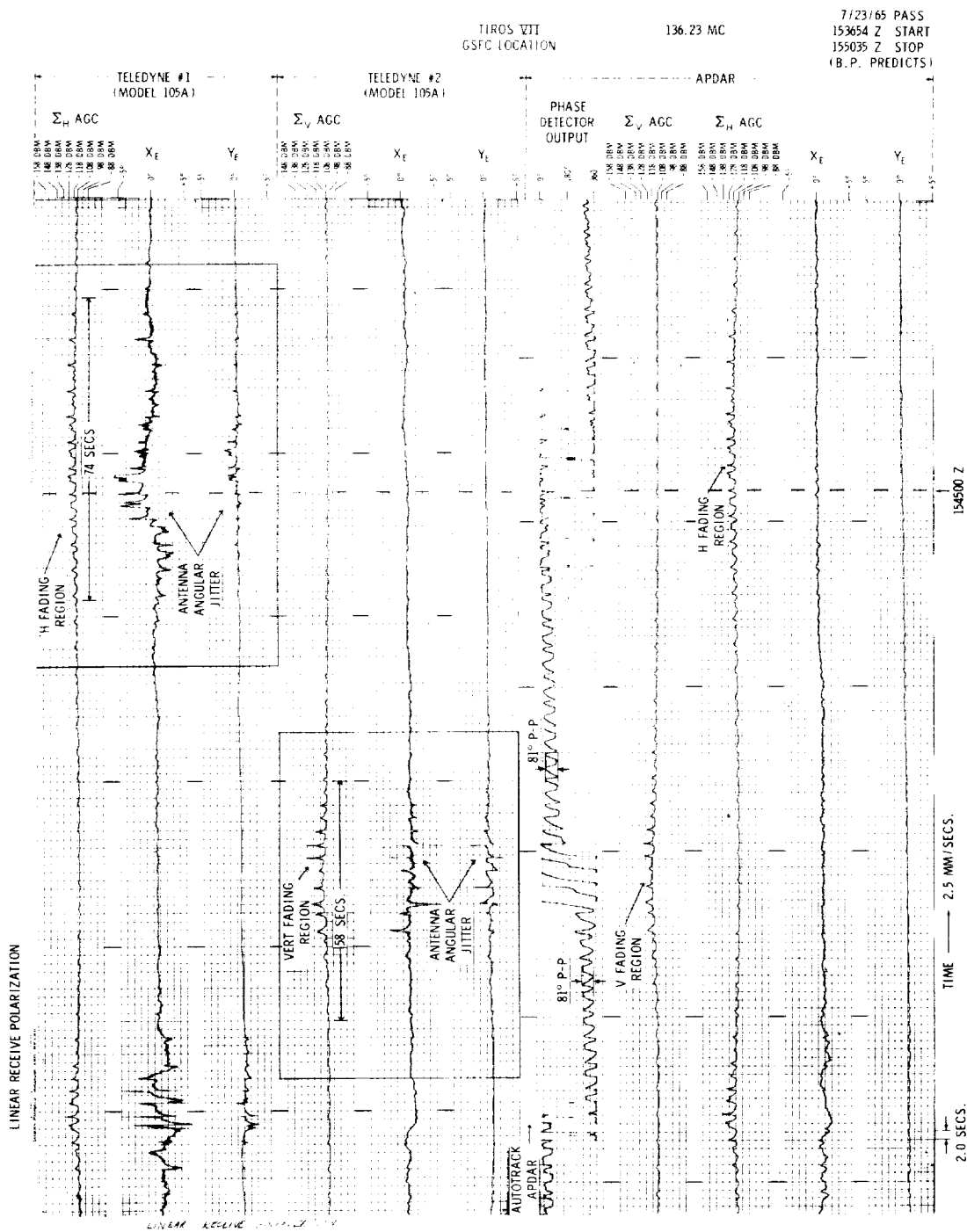


Figure 4-TIROS VII 7/23/65 pass. Comparison of APDAR and conventional autotrack receivers.



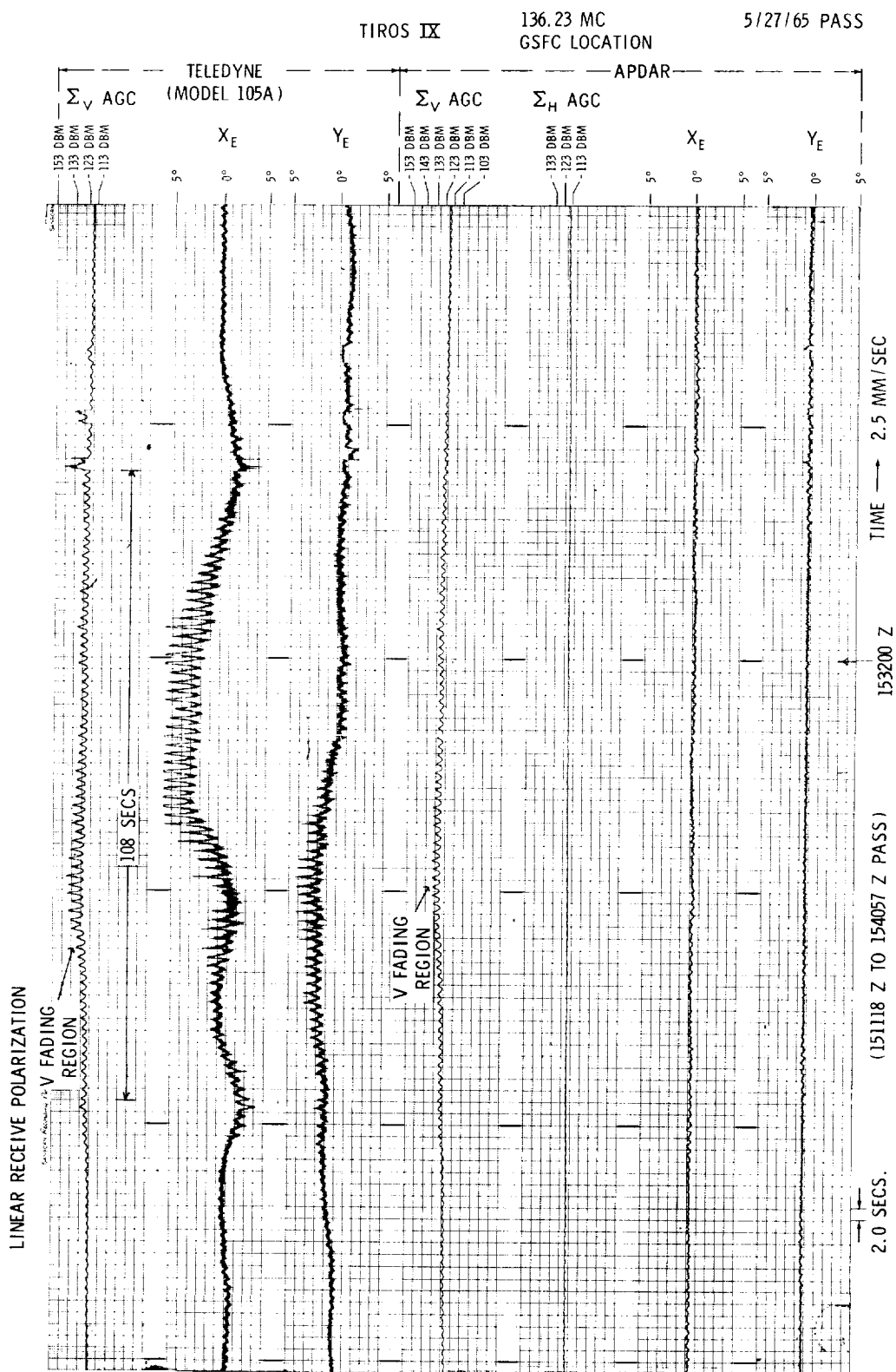


Figure 5-TIROS IX 5/27/65 pass. Comparison of APDAR and conventional autotrack receivers.

TIROS IX  
GSFC LOCATION

136.23 MC

5/28/65 PASS  
START: 150100 Z  
STOP: 153100 Z

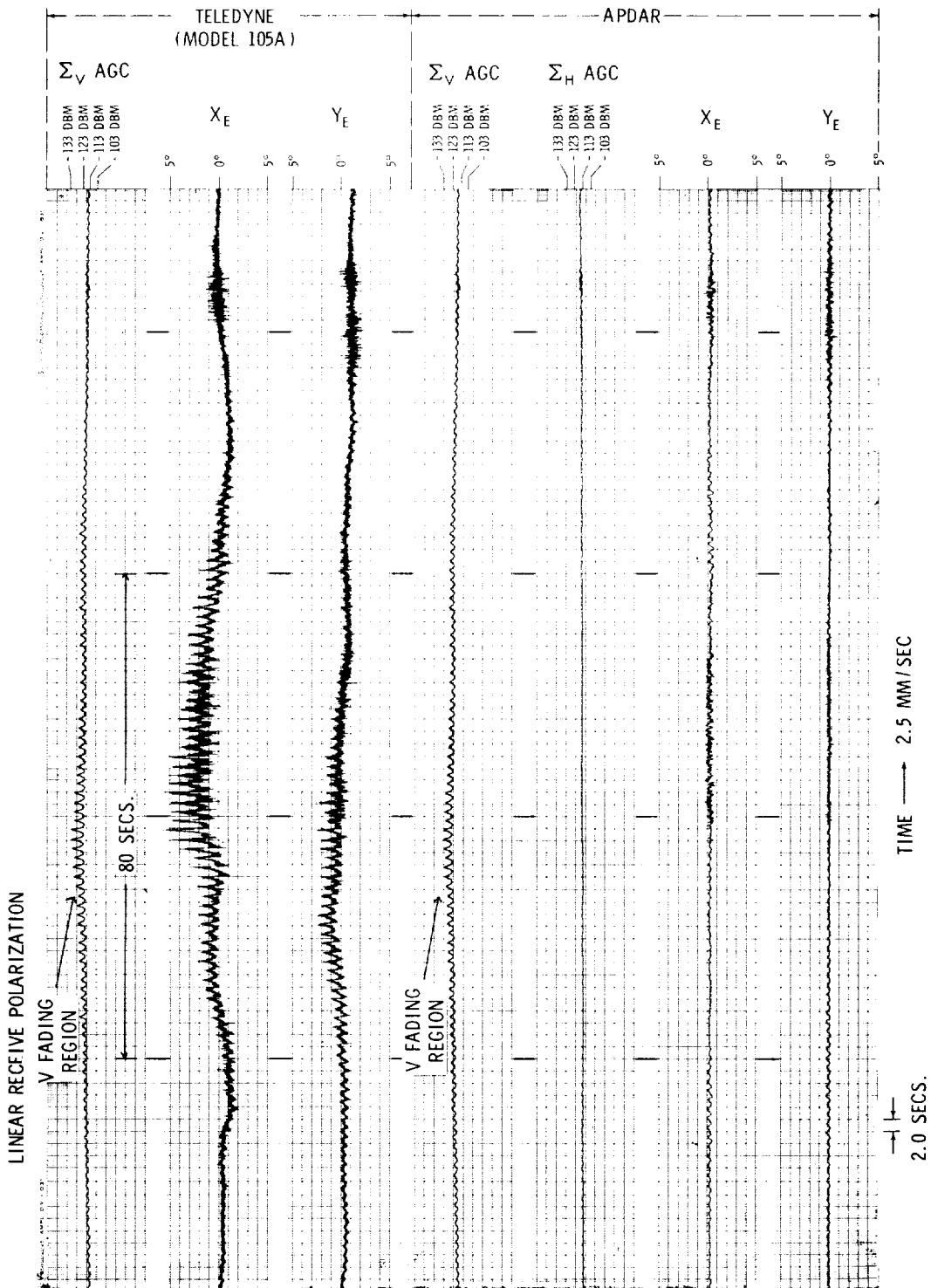


Figure 6-TIROS IX 5/28/65 pass. Comparison of APDAR and conventional autotrack receivers.

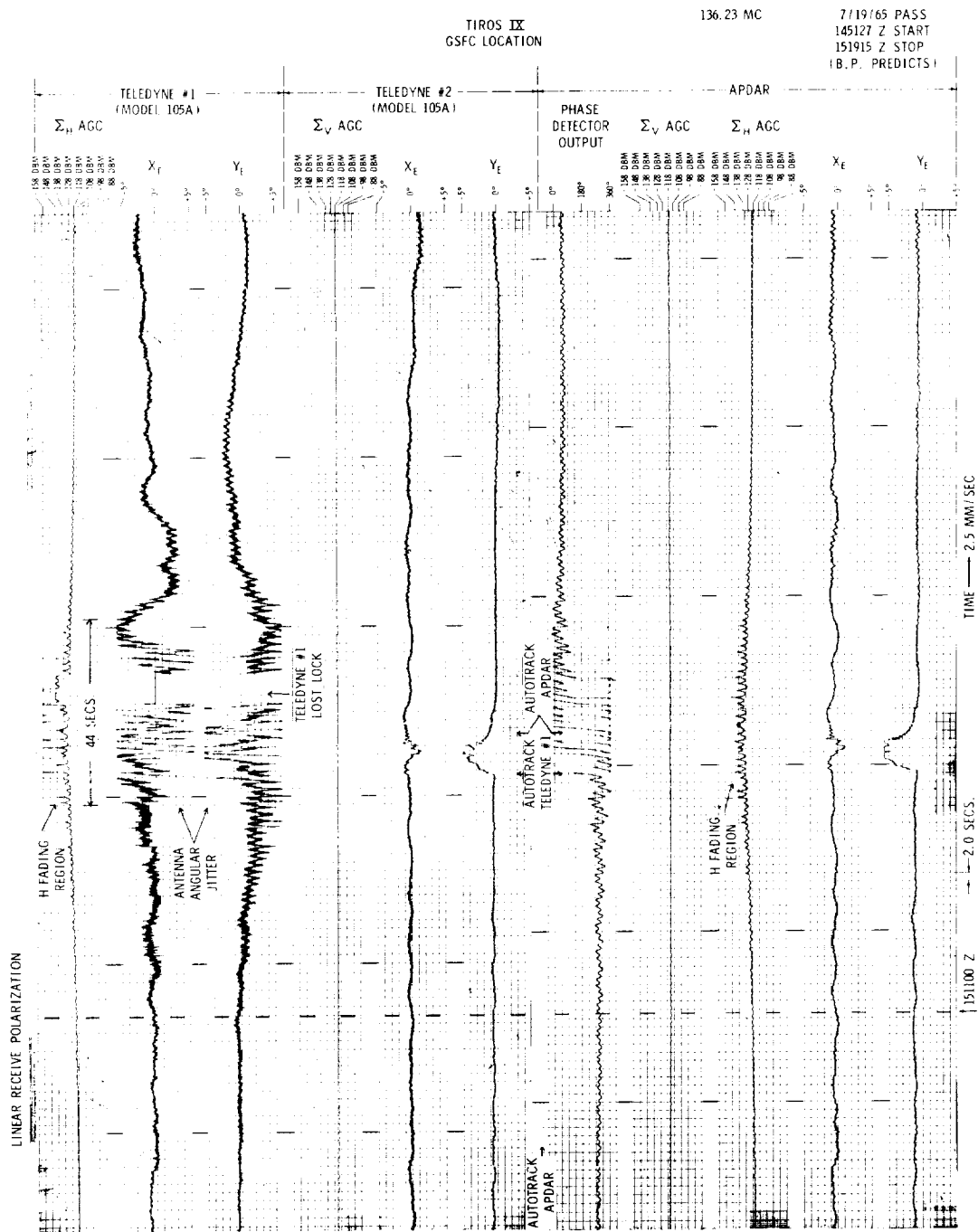


Figure 7-TIROS IX 7/19/65 pass. Comparison of APDAR and conventional autotrack receivers.

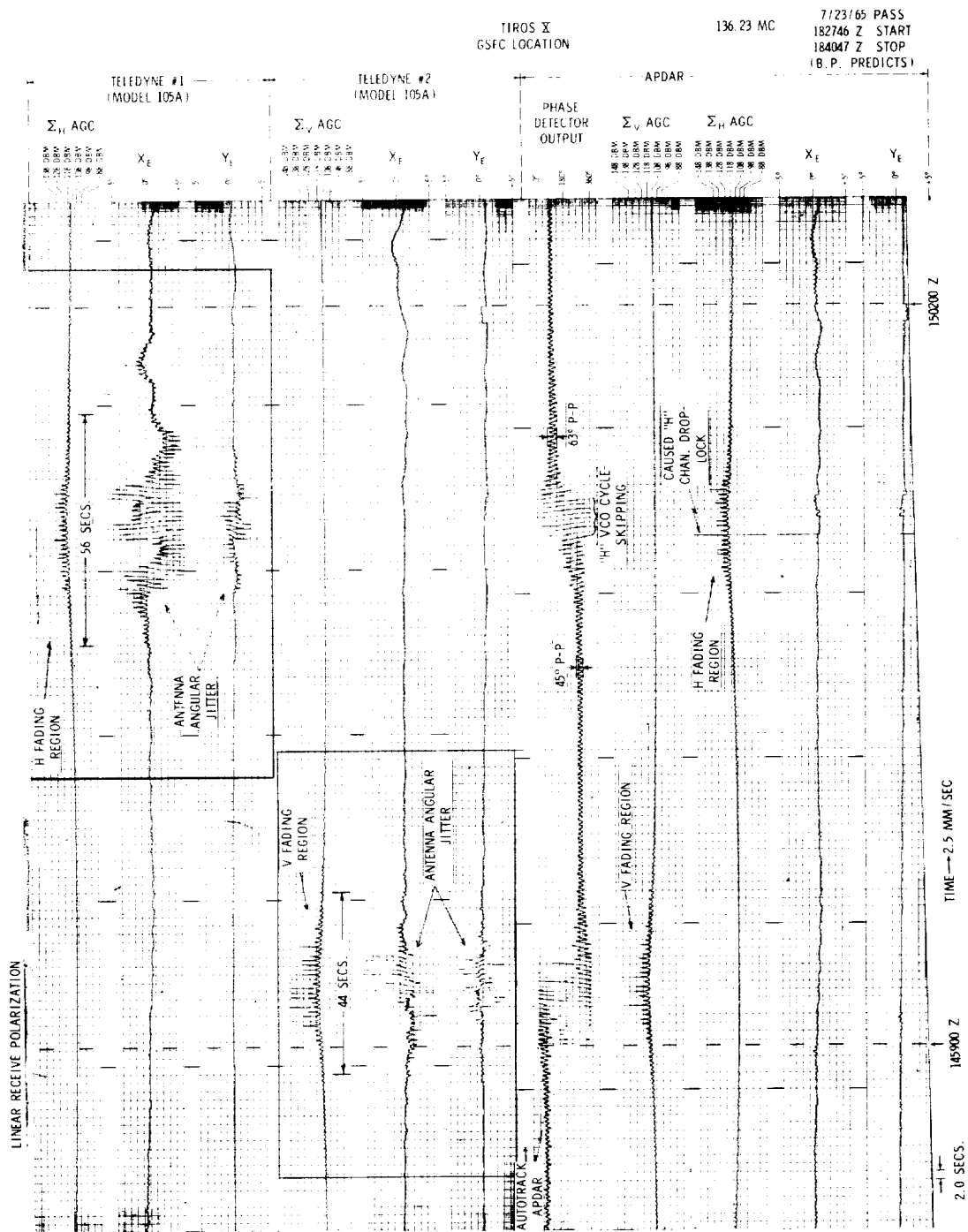


Figure 8-TIROS X 7/23/65 pass. Comparison of APDAR and conventional autotrack receivers.

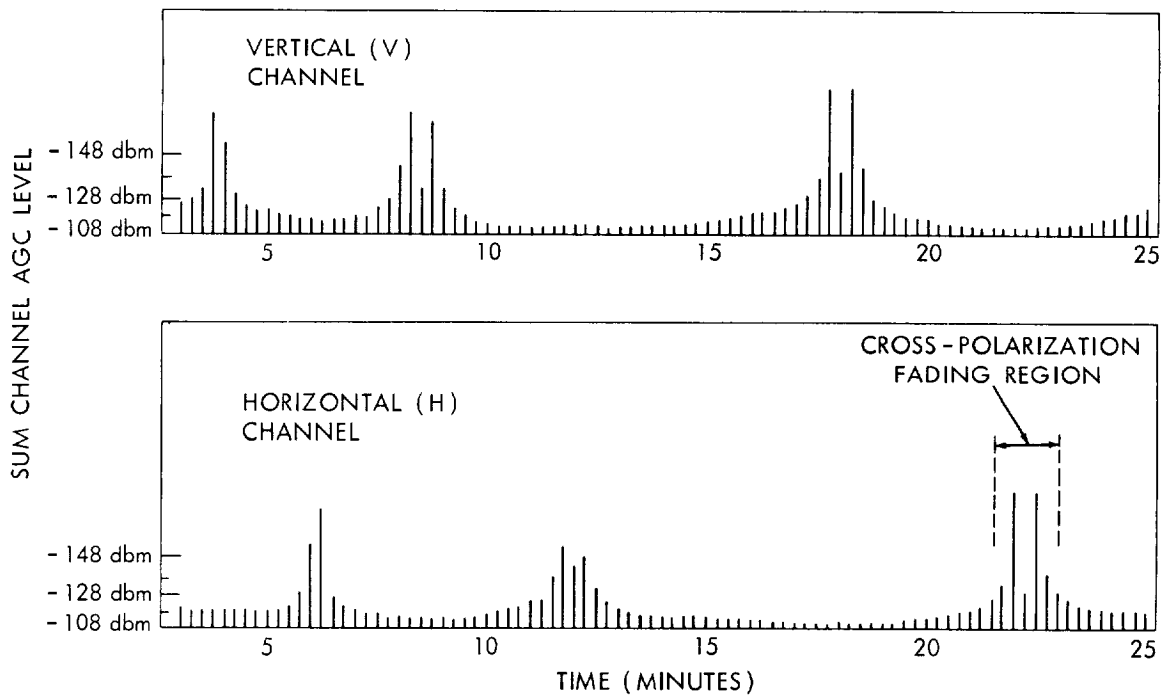


Figure 2-TIROS IX, vertical (V) and horizontal (H) fading characteristics.

channels were essentially not influenced by polarization fading, but the conventional autotrack X- and Y-axis error channels were adversely affected by polarization fading. The error channel jitter caused by fading was large enough, when using a Teledyne receiver for autotrack, to cause excessive antenna angular variations exceeding 10 degrees peak-to-peak. The autotrack function was thereafter quickly transferred by the operator back to APDAR to quiet the system down and prevent loss of receiver lock as well as to prevent possible mechanical damage to the antenna. A case in point is shown in Figure 7 when the Teledyne No. 1 receiver was in autotrack and loss of lock occurred during a fading region.

The performance of APDAR while tracking TIROS VII, IX and X gave less than 1 degree peak to peak (space degrees) of X- and Y-axis error jitter during the fading regions. Such performance represents at least a 10:1 improvement over conventional autotrack performance.

LINEAR RECEIVE POLARIZATION  
(LINEAR XMIT)

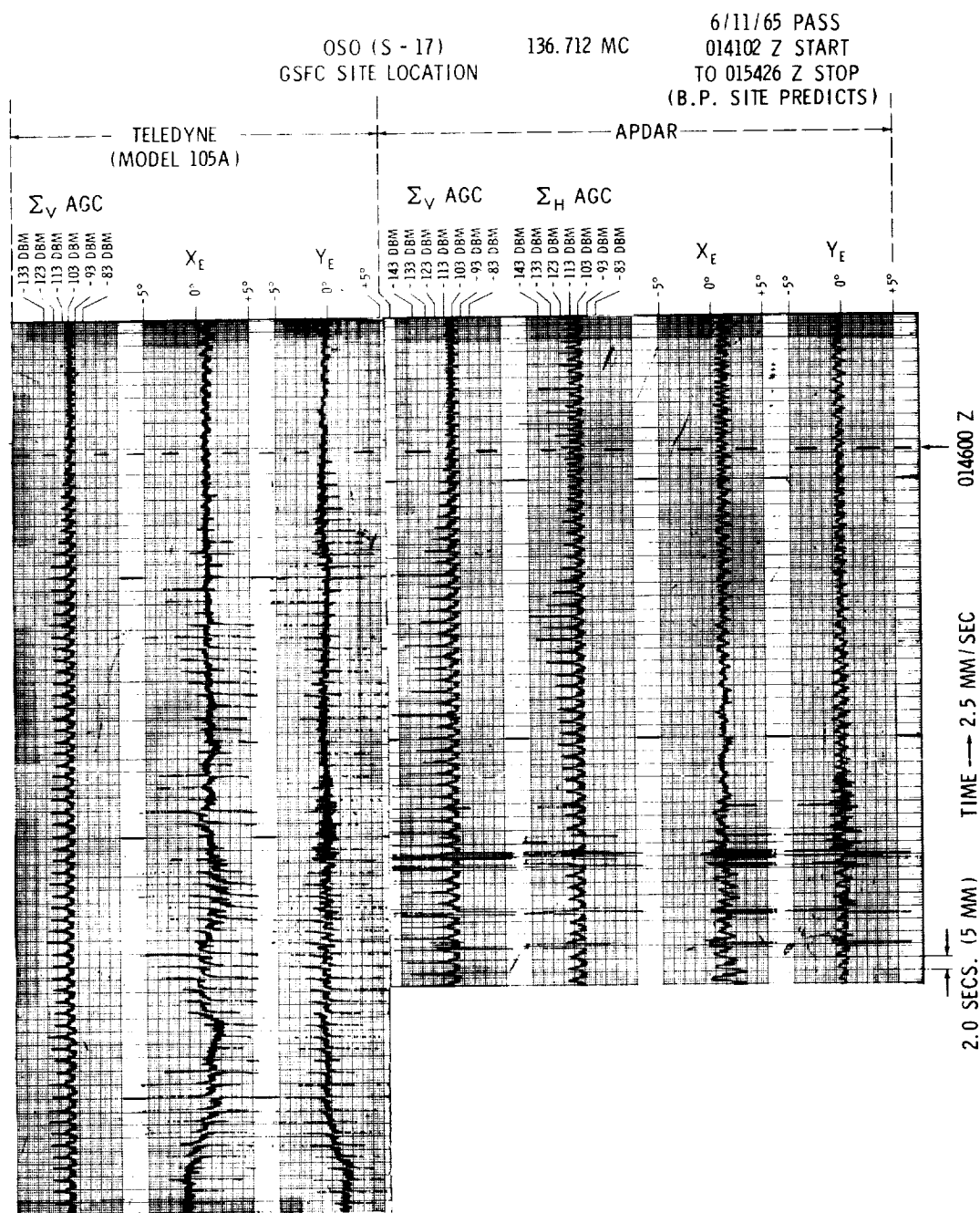


Figure 10-OSO (S-17) 6/11/65 pass. Linear receiving polarization.

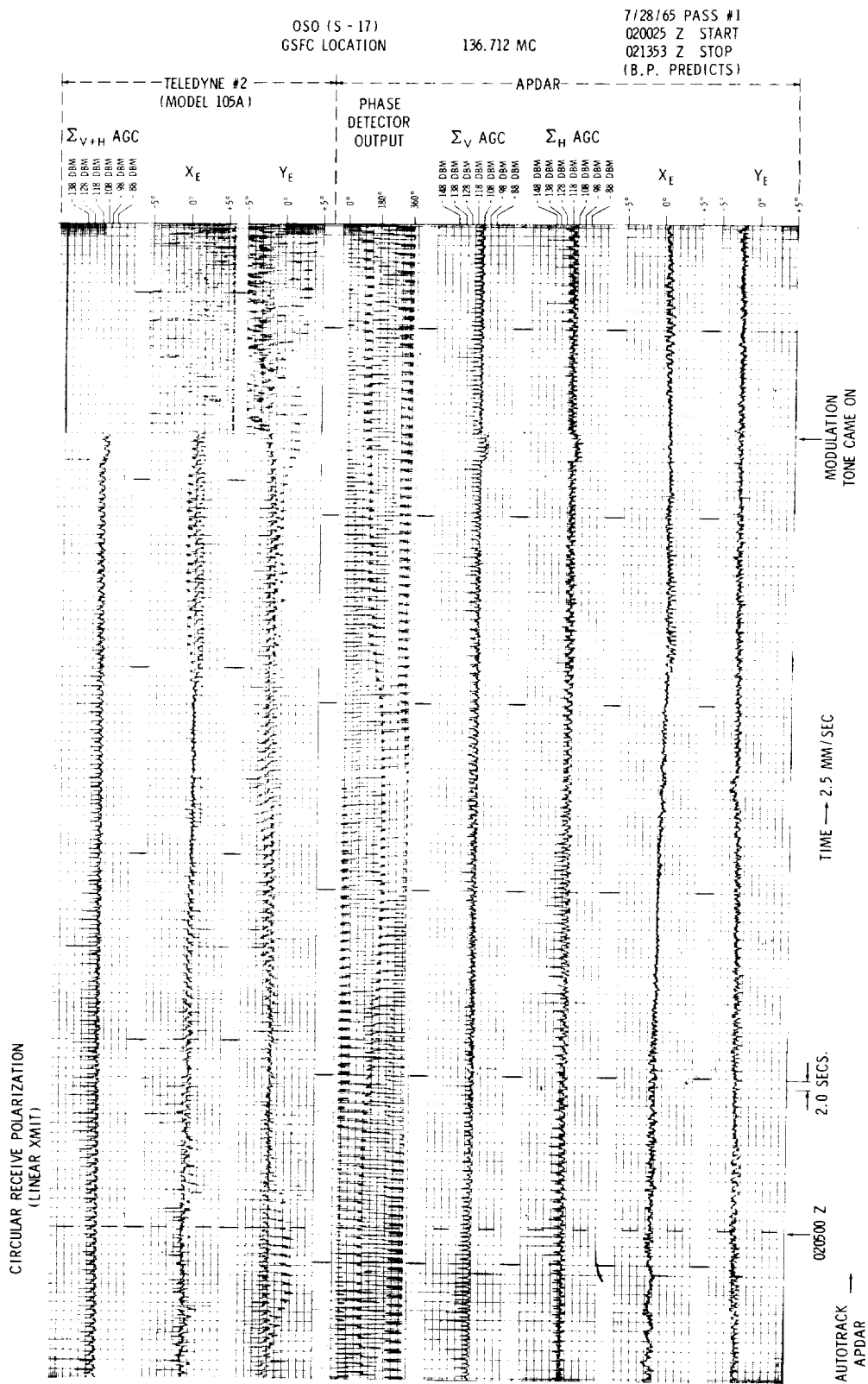


Figure 11-OSO (S-17) 7/28/65 pass No. 1. Comparison of APDAR and conventional autotrack receivers.

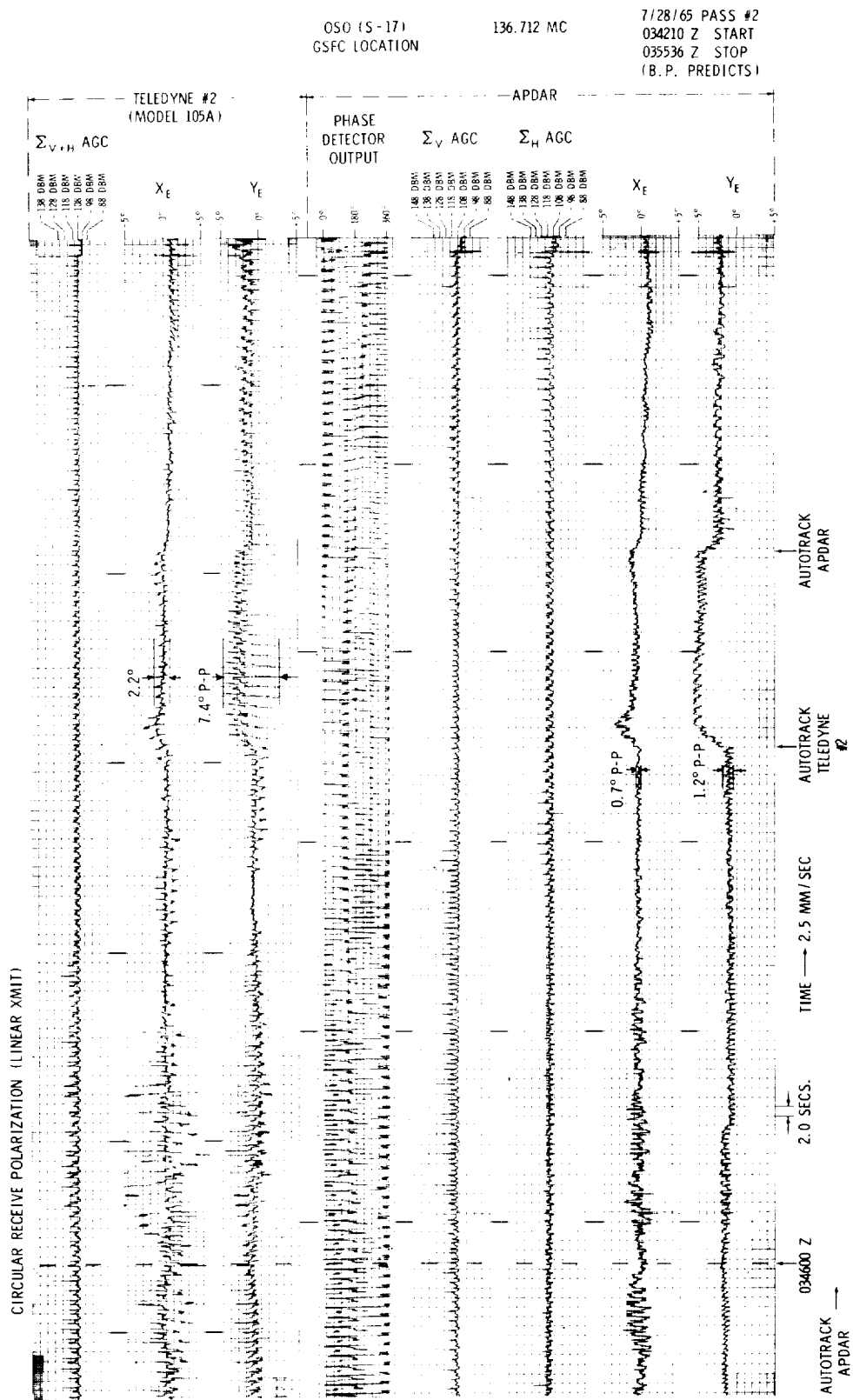


Figure 12-OSO (S-17) 7/28/65 pass No. 2. Comparison of APDAR and conventional autotrack receivers.



The amount of V and H polarization fading during a pass was an appreciable portion of the satellite pass-time and typical combined values range from 18 percent to 42 percent (Table 1).

Table 1  
Percentage Polarization Fading for TIROS VII, IX and X.

Satellite Type	Pass Length (minutes)	Type Polarization Fading	Typical Fading Region Length (seconds)	Fading During Pass (%)	Combined Total Pass Fading (%)
TIROS VII	14	Vertical	58	21	42
TIROS VII	14	Horizontal	74	22	
TIROS IX	29	Vertical	80-108	8	18
TIROS IX	29	Horizontal	44	10	
TIROS X	14	Vertical	44	17	30
TIROS X	14	Horizontal	56	13	

Input V and H signal level fading, ranging in value from 5 db to greater than 30 db, alternates between the V and H channels as revealed by a typical TIROS IX reduced-data AGC recording (Figure 9) showing the fading characteristic.

The TIROS X polarization fading data were similar to those of TIROS IX. Two TIROS X polarization fading regions, resulting in erratic Teledyne auto-track receiver performance in both regions (Figure 8), clearly demonstrate the superior performance of APDAR. Smooth APDAR X-Y error channel outputs are evident in these corresponding regions. The TIROS VII polarization fading data of Figure 4 show similar results for TIROS IX.

#### OSO (S-17) TEST RESULTS

The OSO 30 rpm (nominal) spin rate causes alternate V and H polarization fades as great as 30 db. Figure 10 shows the APDAR sum-channel AGC records; however, APDAR minimizes the effect of the fading since the V and H fades are interdigital and do not occur simultaneously.

The OSO (S-17) satellite transmits linear polarization, thus a circularly polarized receiving mode hookup (Figure 3) was used to obtain optimum performance from the single Teledyne (model 105A) autotrack receiver. The variable phase shifters in the hybrid distribution network were adjusted to a value  $\Delta\theta = 90$  degrees to obtain circular polarization.

The OSO (S-17) recordings (Figures 11 and 12) also clearly demonstrate the superior performance of APDAR, compared to a conventional autotrack receiver, as evidenced by reduced antenna angular jitter. The error channel jitter did not exceed 1 degree peak to peak (space degrees) when utilizing APDAR for autotrack (Figure 11); however, a transfer of the autotrack function from APDAR to Teledyne (Figure 12) resulted in an increase from a value of 1.2 degrees up to 7.4 degrees or an increase of 6.4:1 for the worst case Y-axis error channel.

An interesting event from an operational standpoint is that the Teledyne autotrack receiver lost phase-lock when the OSO (S-17) modulation tone appeared (Figure 11). The received signal was fairly high (about -110 dbm) at that time and continued at this level, as indicated by the APDAR receiver which remained in phase-lock.

A similar STADAN operational difficulty has been experienced with OSO due to a spacecraft modulator that causes an undesirable 7 kc carrier frequency shift. Phase-lock theory indicates that the Teledyne receiver second-order tracking loop is not able to handle this frequency transient as well as the APDAR third-order loop.

## RF PHASE MEASUREMENTS

The design of our existing STADAN autotrack antennas was predicated on maintaining a fixed RF phase relationship between V and H antenna signal components (i.e., manual polarization switching performed in discrete steps of 0 degrees,  $\pm 90$  degrees, or  $\pm 180$  degrees).

The 136 Mc RF phase measurements obtained from this evaluation indicate that the phase-difference,  $\Delta\phi$ , between the V and H antenna RF signals is not constant but varies widely during a pass.

The phase measurement records were obtained by comparing the auxiliary channel V and H voltage controlled crystal oscillator (VCXO) 3.2 Mc output signals in a linear 360 degree (zero crossing) phase detector. This is illustrated in Figures 2 and 3. Both VCXO's must be phase-locked for a phase measurement.

A typical TIROS X record excerpt (Figure 8) indicates that the RF phase-difference,  $\Delta\phi$ , varies sinusoidally with satellite spin (approximately 10 rpm) over the range of about 45 degrees peak to peak to 63 degrees peak to peak. This phase variation is probably permissible, however, because the performance of the conventional autotrack receiver was not degraded.

The phase difference ( $\Delta\phi$ ) varied at a rate approximately equal to 0.8 cps for TIROS X. The APDAR auxiliary phase-lock loop 10 cps tracking loop bandwidth (10 percent of main tracking bandwidth, 100 cps) used in this evaluation is more than sufficient to follow this phase rate.

It is observed that an H-AGC channel deep-fade point occurred (Figure 8, TIROS X) that caused the APDAR auxiliary H-tracking loop to lose phase-lock and momentarily skip cycles. The auxiliary H-channel tracking loop again went into phase lock near the end of the H-fading region, thereby again providing additional phase data. However, APDAR gave smooth tracking through the H-channel fading region, since the V-channel was uniform.

The TIROS VII RF phase measurements (Figure 4) indicate larger phase excursions ( $\Delta\phi = 81$  degrees peak to peak) but even these high values did not significantly degrade conventional autotrack receiver performance. The TIROS VII values of  $\Delta\phi$  varied at a slower rate than TIROS X, a typical rate being 0.3 cps.

The OSO (S-17) satellite was spinning at about 30 rpm (compared to approximately 10 rpm for TIROS series) resulting in a much higher phase rate for  $\Delta\phi$ . Also, OSO is transmitting linear polarization, which increases the apparent phase rate because the APDAR auxiliary V and H phase-lock channels separately track the respective V and H radio frequency signals from the antenna.

Values of  $\Delta\phi$  for OSO vary widely between the 360 degrees limits, but the maximum phase rate was only about 900 degrees/second, corresponding to an equivalent rate of 2.5 cps. The OSO phase data must be interpreted carefully since the 0 to 360 degree phase detector saw-tooth return (or reset) transient is also present in each satellite spin period.

The APDAR 10 cps auxiliary channel tracking loop bandwidth used in this evaluation test also appears to be wide enough to adequately track the OSO maximum RF phase rate.

Additional V and H channel RF phase measurements were obtained by tracking IMP-C (Figure 13), but the maximum phase rate was about 180 degrees/second which is equivalent to only 0.5 cps. Values of  $\Delta\phi$  ranged from 72

IMP C  
GSFC LOCATION  
136.5 MC

8/6/65 PASS  
152251 Z START  
002954 Z STOP  
(B.P. PREDICTS)

IMP C  
GSFC LOCATION  
136.5 MC

8/12/65 PASS  
155110 Z START  
055622 Z STOP  
(B.P. PREDICTS)

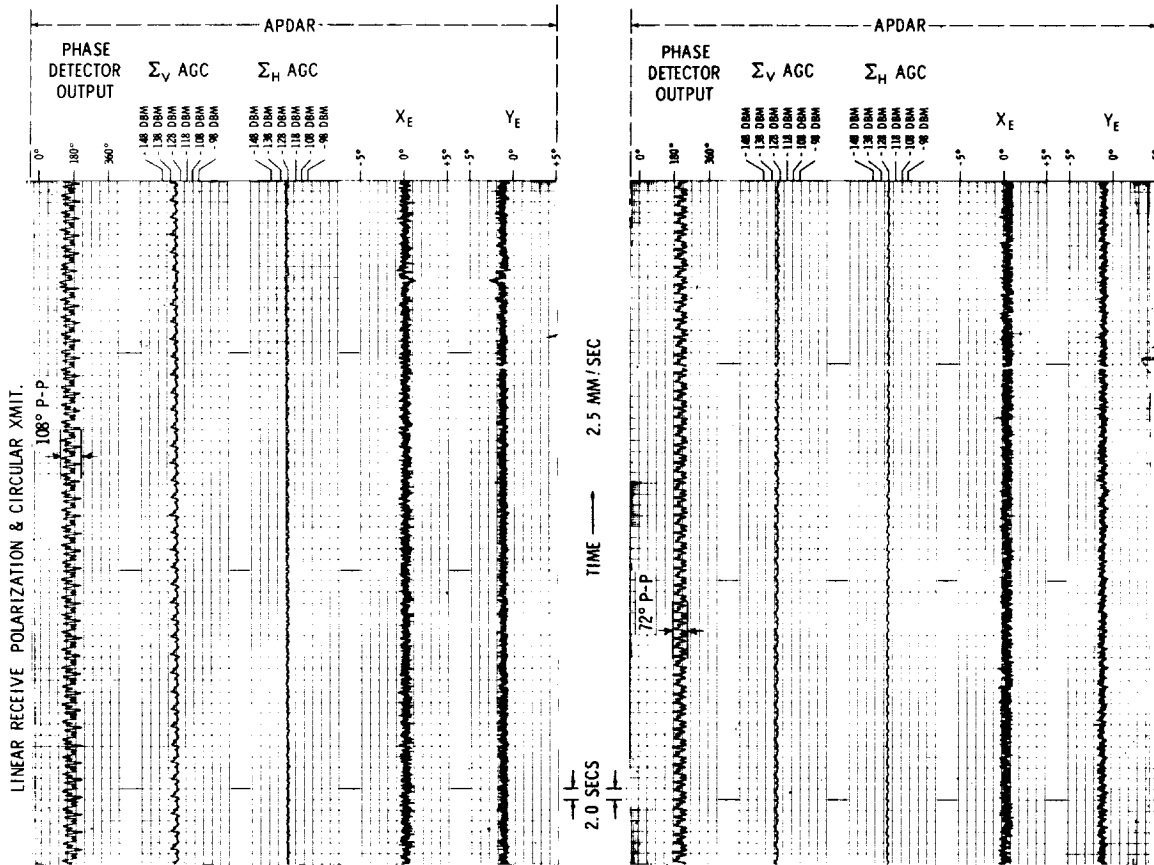


Figure 13-IMP C APDAR vertical (V) and horizontal (H) phase data.

degrees peak to peak to 108 degrees peak to peak for the two IMP passes, and the phase excursion waveforms were remarkably uniform.

The APDAR auxiliary channel 10 cps tracking bandwidth used for this test is also more than adequate to properly track the IMP-C RF phase rate.

#### BORESIGHT ANTENNA ROTATION TESTS

The aspect changes of an earth-orbiting satellite causes the ground-station received RF polarization to vary frequently during a pass, from circular to linear polarization, even though a circularly polarized transmitting antenna is used. This occurs because a typical circularly polarized spacecraft transmitting antenna is actually polarized linearly over an approximate 45 degree angular region perpendicular to the circular polarization axis (Figure 14).

Therefore, a linearly polarized ground-station receiving antenna, optimized by being set to receive only the transmitted circular polarization, experiences cross-polarization fading at frequent intervals during a satellite pass (Figure 9) when the transmitted wave becomes linearly polarized.

A rotating linearly polarized 136.5 Mc boresight antenna (dipole) was utilized to simulate the effect of polarization rotation caused by satellite aspect changes (Figure 15). The linearly polarized dipole was thus slowly rotated by a manually controlled motor to simulate the effect of linear cross-polarization on autotrack performance occurring when the spacecraft linearly polarized 45 degrees region (Figure 14) is pointed toward the ground-station.

The APDAR receiver and a single Teledyne (Model 105A) autotrack receiver were connected so that APDAR received the V and H polarization directly, whereas the Teledyne unit operated from combined V and H signals (Figure 3) provided by the hybrid distribution network. The hybrid phase shifters ( $\Delta\theta_1$ ,  $\Delta\theta_2$ , and  $\Delta\theta_3$ ) were initially adjusted so that the Teledyne receiver obtained an elliptically polarized signal (ellipticity ratio = -20 db) which, for all practical purposes, corresponds to linear polarization. Both receivers were phase-locked to the boresight antenna signal source (unmodulated carrier) with the APDAR receiver performing the autotrack function.

These simulated tests clearly demonstrated that the conventional autotrack receiver experienced a severe error-channel 8.5 degree peak to peak (space degrees) phase transient (Figure 16, Teledyne Y-axis Sanborn recording) at the 20 db null point shown on the Teledyne sum-channel AGC record. The reduced Teledyne receiver X-axis variation is due to the fact that the phase shifter,

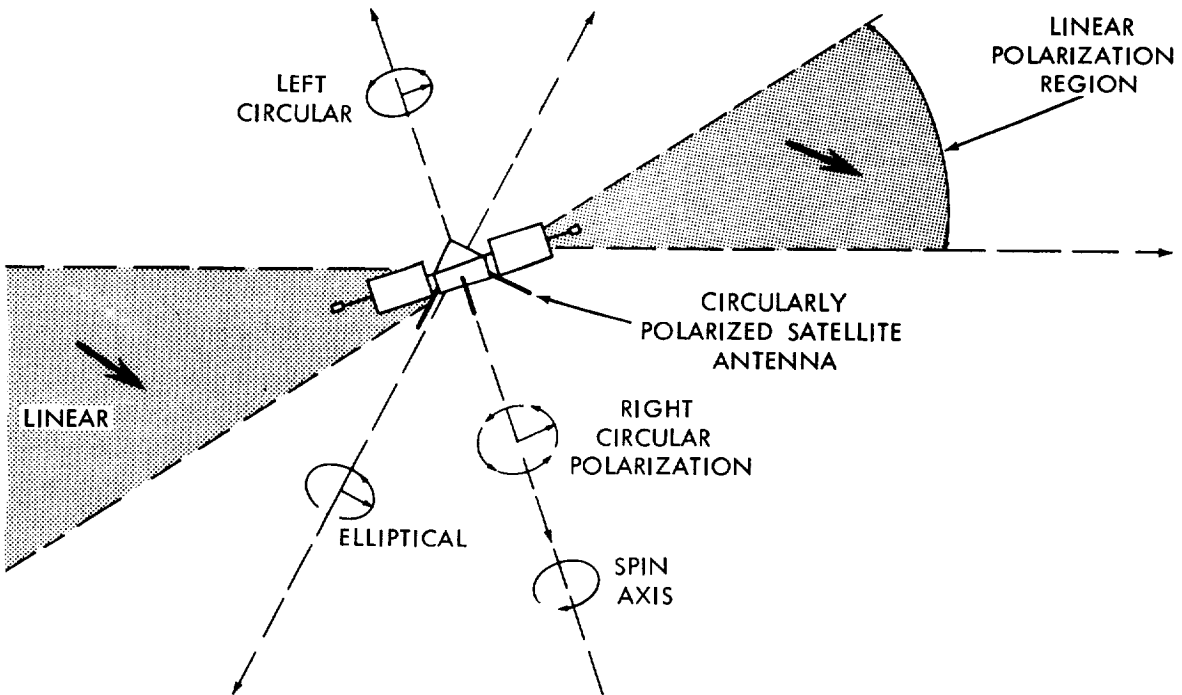


Figure 14-Variations transmitted by a circularly polarized satellite antenna.

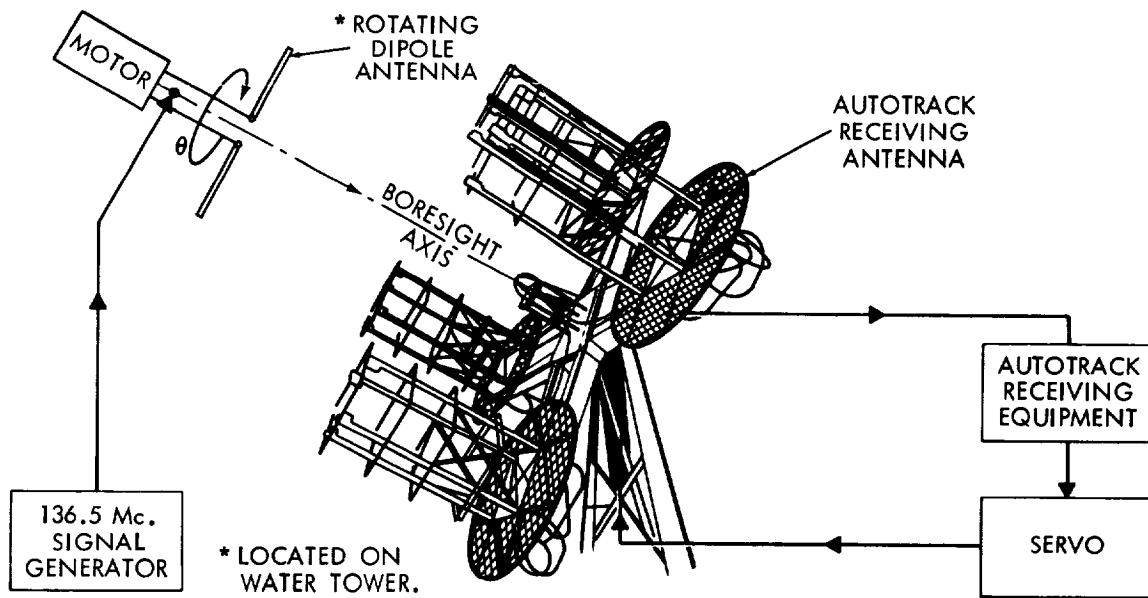


Figure 15-Boresight antenna test to simulate satellite polarization fading.

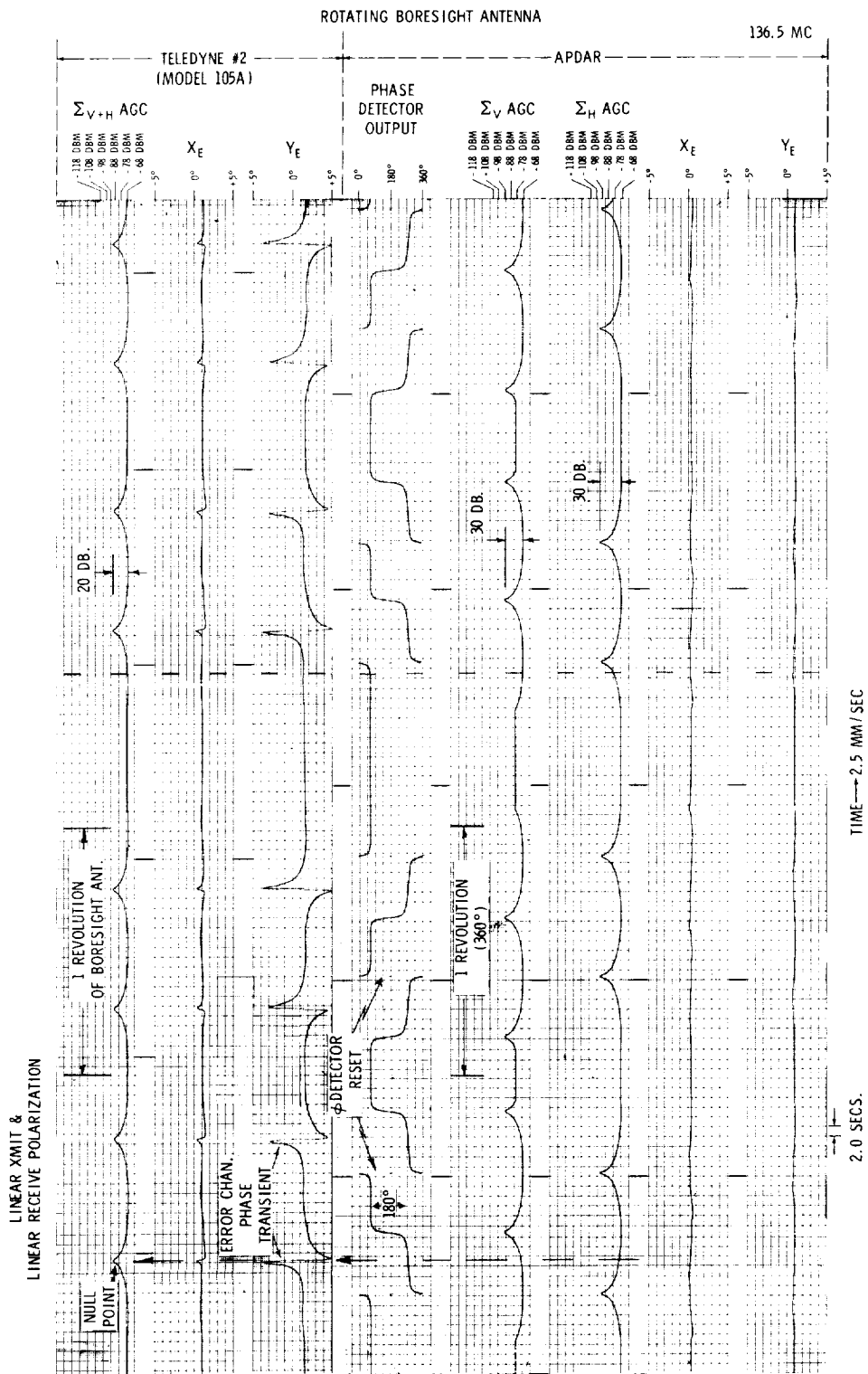


Figure 16-Boresight antenna rotation test. Linear polarization to Teledyne autotracking receiver.

$\Delta\theta_1$ , was adjusted such that the X-axis difference channel signal was more nearly circularly polarized, rather than being linearly polarized.

The boresight antenna experiment thus confirms that cross-polarization is the mechanism that can cause excessive angular jitter of the autotrack antenna observed.

The performance of APDAR during the simulation tests was superior to that of conventional autotrack, as shown by the smooth X-Y error-channel recordings (Figure 16) where the angular error was less than 0.5 degree peak to peak, even though the V and H sum levels experienced 30 db nulls at the cross-polarization points.

An additional boresight antenna test was performed to simulate ideal conditions where true circular polarization was provided to the conventional autotrack receiver (Figure 3, hybrid distribution network phase shifters,  $\Delta\theta_1 = \Delta\theta_2 = \Delta\theta_3 = 90^\circ$ ). The APDAR unit again performed the autotrack function.

The performance of the conventional autotrack receiver under ideal conditions was thus found to be comparable to the APDAR performance (Figure 17) where both receivers had X-Y axis difference channel angular errors of less than 0.5 degrees peak to peak (space degrees). Unfortunately, the satellite transmitting antenna does not always provide these ideal conditions.

## CONCLUSIONS

The 136 Mc satellite tracking evaluation tests described herein clearly show the superiority of an autotrack system such as APDAR that utilizes an automatic polarization tracking feature (pre-detection diversity combining) in lieu of a fixed receiving polarization.

It was demonstrated that polarization fading, sufficient to seriously degrade autotrack performance, occurs either with circular or linear polarization transmitted by the spacecraft.

The autotrack receivers utilized for comparison with APDAR were typical STADAN units and similar performance would have been obtained with any unit of a similar type, regardless of the manufacturer.



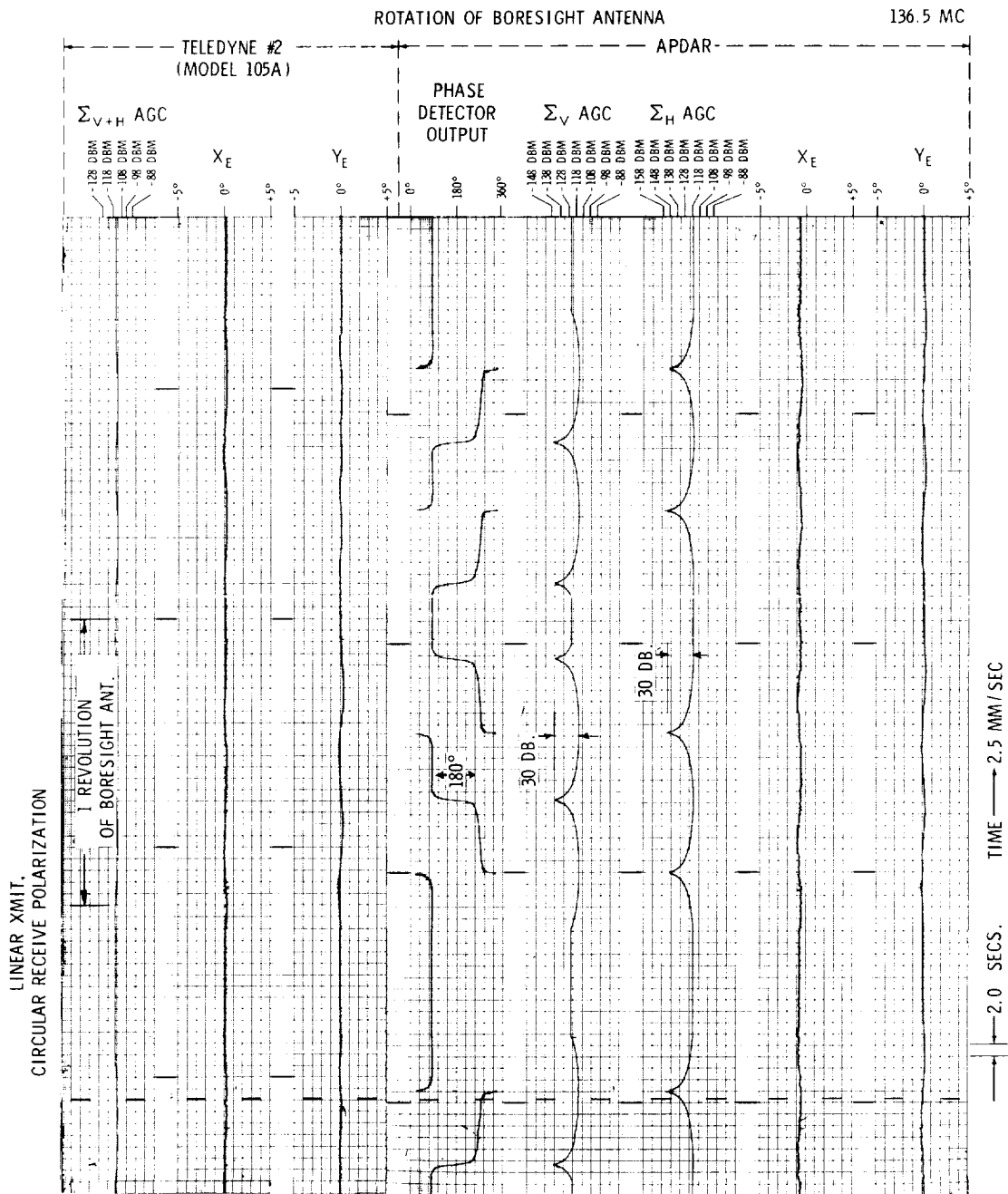


Figure 17-Boresight antenna rotation test. Circular polarization to Teledyne autotrack receiver.

## ACKNOWLEDGMENT

The author wishes to acknowledge the assistance of Mr. Wilfred B. Hillstrom during the installation and testing of the autotrack receiving equipment. In addition, the effort of Mr. Richard Vale (coop student, University of Detroit) is acknowledged for the preparation and mounting of the numerous Sanborn recording excerpts.

Also, the author is grateful for the use of the 136 Mc phase-array autotrack antenna provided by the Antenna Systems Branch, Advanced Development Division.

## REFERENCES

1. Rhodes, D. R., "Introduction to Monopulse," New York: McGraw-Hill Book Co., Inc., 1959.
2. Brennan, D. G., "Linear Diversity Combining Techniques," Proc. IRE, 47(6):1075-1102, June 1959.
3. Laughlin, C. R., "The Diversity-Locked Loop-Cohcrent Combiner," IEEE Trans. Space Elect. Telem. SET 9(3):84-92, September 1963.
4. Taylor, R. E., "1-10Kmc Advanced Polarization Diversity Autotrack Receiving System," Greenbelt, Maryland: Goddard Space Flight Center, Monthly Research and Advanced Technology Development Activity Report, Number 7 for April 1963, I-230-63-19, April 25, 1963 (Official use only).